Activation of the Sonic Hedgehog Signaling Controls Human Pulmonary Arterial Smooth Muscle Cell Proliferation in Response to Hypoxia

Guansong Wang[a,b,*], **Zhiyuan Zhang**[a,c,*], **Zhi Xu**[a], **Hongjin Yin**[a], **Li Bai**[a], **Zhuang Ma**[c], **Mark A. DeCoster**[d], **Guisheng Qian**[a,#], and **Guangyu Wu**[b,#]

[a] Institute of Respiratory Diseases, Xinqiao Hospital of the Third Military Medical University, Chongqing 400037, P. R. China

[b] Department of Pharmacology and Experimental Therapeutics, Louisiana State University Health Sciences Center, New Orleans, Louisiana 70112, USA

[c] Department of Respiratory Diseases, General Hospital of Shenyang, Shenyan 110016, P. R. China

[d] Biomedical Engineering and Institute for Micromanufacturing, Louisiana Tech University, Ruston, LA 71272, USA

Abstract

The hedgehog signal pathway plays a crucial role in the angiogenesis and vascular remodeling. However, the function of this pathway in the pulmonary vascular smooth cell proliferation in response to hypoxia remains unknown. In this study, we have demonstrated that the main components of the hedgehog pathway, including sonic hedgehog (SHH), patched1 (PTCH1), smoothened (SMO), GLI and hypoxia-inducible factor 1 (HIF1) are expressed in the human pulmonary arterial smooth muscle cells (HPASMCs). Interestingly, hypoxia significantly enhanced the expression of SHH and HIF1, facilitated the translocation of GLI1 into the nuclei, and promoted the proliferation of HPASMCs. Furthermore, direct activation of the SHH pathway through incubation with the purified recombinant human SHH or with purmorphamine and SAG, two Smo agonists, also enhanced the proliferation of HPASMCs. Importantly, the treatment with anti-SHH and anti-HIF1 antibodies or cyclopamine, a specific SMO inhibitor, markedly inhibited the nuclear translocation of GLI1 and cell proliferation in the HPASMCs induced by hypoxia and activation of the SHH pathway. Moreover, the treatment with cyclopamine increased apoptosis in the hypoxic HPASMCs. These data strongly demonstrate for the first time that the SHH signaling plays a crucial role in the regulation of HPASMC growth in response to hypoxia.

Keywords

anoxia; hedgehog signal pathway; sonic hedgehog; GLI; cell proliferation; human pulmonary arterial smooth muscle cells

[#]Corresponding author: Guangyu Wu: Tel: +1 504-568-2236; Fax: 504-568-2361; gwu@lsuhsc.edu, Guisheng Qian: Tel.: +86 23 6522 2936; fax: +86 23 6521 1653; qiangs@mail.tmmu.com.cn.
[*]These authors contributed equally to this work.

1. Introduction

It has been well documented that hypoxia enhances the progress of vascular remodeling in a number of human diseases, including atherosclerosis, pulmonary artery hypertension and chronic obstructive pulmonary disease [1–4]. During vascular remodeling, vascular smooth muscle cells (VSMCs) undergo proliferation, hypertrophy, migration, and/or apoptosis [5–9]. The molecular mechanisms responsible for these alterations under the hypoxic condition have been extensively studied and indeed, a number of signaling pathways, such as the JAKs/STATs [10,11], PI3 kinase/Akt [12,13], and mitogen-activated protein kinase pathways [14,15], have been demonstrated to play important roles in the regulation of VSMC phenotypes.

Hedgehog (HH) proteins are secreted glycoproteins that bind to the plasma membrane receptor Patched (PTCH) [16–20]. PTCH1 is a twelve-transmembrane receptor that negatively regulates the function of Smoothened (SMO). SMO possess a seven-transmembrane domain, a characteristic of the superfamily of G protein-coupled receptors, and recent studies have demonstrated that the function of SMO may be indeed mediated through coupling to heterotrimeric G proteins [21,22]. Under the normal condition, the function of SMO is suppressed by PTCH1. Upon HH binding to PTCH1, the inhibitory effect of PTCH1 on SMO will be released resulting in the activation of SMO and the GLI family of transcriptional factors, initiating expression of target genes including those associated with cell cycle progression [23–25]. Three members of the hedgehog family, Sonic hedgehog (SHH), Indian hedgehog, and Desert hedgehog and three GLI proteins, GLI1, GLI2 and GLI3 have been identified. The SHH signaling pathway was first discovered to control the segmentation patter of *Dorsophila* and has been shown to regulate cell migration, proliferation, and apoptosis in several cell lines, such as cancer cells, neuron cells, and aortic VSMCs [9,26–33]. Particularly, the activation of the SHH signaling pathway is associated with retinal neovascularization, neural progenitor proliferation and muscle regeneration under the hypoxic condition [34–36]. It has also been demonstrated that nuclear translocation of GLI1 induces the expression of several genes, such as cyclin D, cyclin E and myc, which all are involved in the regulation of cell proliferation [37–39].

Hypoxia has been demonstrated to activate the SHH pathway in cardiomyoblast cells, neurons, astrocytes, and neural progenitor cells [35,40–43]. Hypoxia has also been demonstrated to induce the expression of SHH which is dependent on hypoxia-inducible factor-1 (HIF1), a transcription factor that modulates a variety of gene expression [40,42,44,45]. However, the function of the SHH signaling pathway in the human pulmonary arterial smooth muscle cells (HPASMCs) has not been studied under the normal and hypoxia conditions. In the present study, we have demonstrated that hypoxia markedly activates the SHH signaling pathway in the adult HPASMCs which contributes to the enhanced cell proliferation of the HPASMCs.

2. Materials and methods

2.1. Materials

Antibodies against Shh (C9C5, #2207) were purchased from Cell Signaling Technology (Danvers, MA). Antibodies against and GAPDH (0411, sc-47724), PTCH1 (sc-6147), GLI1 (H-300, sc-20687) and HIF1α (H-206, sc-10790) and thyl-N′-(3-pyridinylbenzyl)-N′-(3-chlorobenzo[b]thiophene-2-carbonyl)-1,4-diaminocyclohexane (SAG) were obtained from Santa Cruz Biotechnology, Inc. (Santa Cruz, CA). Antibodies against TATA binding protein (TBP) was from Abcam ([1TBP18], #ab818, Cambridge, MA). Recombinant human SHH amino terminal peptide was from R&D Systems (Abingdon, UK). Cyclopamine (CyA) was from Biomol International (Biomol Research Laboratories, Plymouth Meeting, PA). SuperSignal West Pico Chemiluminescent Substrate Kits (Horseradish peroxidase (HRP)-conjugated goat anti-rabbit IgG luminal/enhancer solution stable peroxide solution) were from

Thermo Fisher Scientific (Rockford, IL). Secondary antibodies were from Amersham Biosciences (Little Chalfont, UK). Apoptosis Assay Kit was from Molecular Probes (Invitrogen, Eugene, OR). The SYBR PrimeScript RT-PCR kit was from TaKaRa Biotechnology (Dalian, China). All other materials were described elsewhere [46].

2.2. Cell culture

The HPASMCs were purchased from ScienCell Research Laboratories (Carlsbad, CA, USA) and cultured in smooth muscle cell medium (SMCM) supplemented with 2% fetal bovine serum (FBS), 100 U/ml penicillin, 100 μg/ml streptomycin, and 1% smooth muscle cell growth supplement (SMCGS, No. 2415 from ScienCell Research Laboratories, Carlsbad, CA, USA). The final concentrations of SMCGS components are bovine serum albumin (BSA) 10 μg/ml, apo-transferrin 10 μg/ml, insulin 5 μg/ml, FGF-2 2 ng/ml, IGF-I 2 ng/ml and hydrocortisone 1 μg/ml. The HPASMCs were used at passages 4–10 in our experiments.

2.3. HPASMC exposure to hypoxia and pretreatments

Hypoxic culture conditions defined as 3% O_2 were created in an oxygen-regulated cell culture incubator (Heraeus, Germany). Subconfluent HPASMCs were starved in SMCM with 0.4% FBS for at least 24 h and then incubated under either hypoxic or normoxic conditions for various periods of time.

For the pretreatment of the HPASMCs, the cells were preincubated with CyA (5 μM for 2 h), tomatidine (Tom) (5 μM for 2 h), SHH (1.0 μg/ml for 24 h), purmorphamine (Pur) (4 μM for 24 h), SAG (100 nM for 24 h), anti-SHH antibodies (1 μg/ml for 24 h) or anti-HIF1 antibodies (1 μg/ml for 24 h) and then subjected to hypoxia.

2.4. Measurement of SHH in the culture medium of hypoxic HPASMCs

The concentrations of SHH in the culture medium of hypoxic HPASMCs were measured by using an ELISA kit according to the manufacturer's instructions (R&D Systems) and the cells were cultured on 96-well, flat bottom, and EIA/RIA plates (Corning, NY, USA). A standard curve was generated for each experiment using known concentrations of SHH from 0 to 10,000 pg/ml. The concentration of SHH in the conditioned media fell with the linear range of the standard curve and thus, the SHH concentration in the media was calculated from the standard curve by interpolation.

2.5. Quantitative real-time RT-PCR

Total RNAs were extracted from the HPASMCs using TRIzol reagent (Invitrogen, Carlsbad, CA) according to the manufacturer's instruction. Six μg of total RNAs were used for cDNA synthesis with the SuperScript first-strand synthesis system for RT-PCR (Invitrogen). Quantitative real-time RT-PCR was carried out using the Rotor Gene (model RG-6000; Corbett Research, Sydney, Australia) and the SYBR green PCR kit. The primers used were: For SHH, forward primer: 5′-TCCAGAAACTCCGAGCGATTTAAG-3′ and reverse primer: 5′-CACTTCCTGGCCACTGGTTCA-3′; For PTCH1, forward primer: 5′-CCACAGAAGCGCTCCTACA-3′ and reverse primer: 5′-CTGTAATTTCGCCCCTTCC-3′; For Smoothened (SMO), forward primer: 5′-ACGAGGACGTGGAGGGCTG-3′ and reverse primer: 5′-CGCACGGTATCGGTAGTTCT-3′; For GLI1, forward primer: 5-GGGATGATCCCACATCCTCAGTC-3 and reverse primer: 5-CTGGAGCAGCCCCCCCAGT-3; For GLI2, forward primer: 5′-ACACGGGCTTTGGTCTCA-3 and reverse primer: 5′-CCCTTGGGCATAGCTTCT-3′. For GLI3, forward primer: 5′-ACCATGGGCTTCAGTCAG-3′ and reverse primer: 5′-CAATCTGCACGCCTTCTA-3′; For GAPDH, forward primer: 5′-AACGACCCCTTCATTGAC-3′ and reverse primer: 5′-TCCACGACATACTCAGCAC-3′.

The following program was used: denaturation at 95 °C for 5 min and 40 cycles consisting of denaturation at 95 °C for 10 sec, annealing at 56–65 °C for 5 sec, and extension at 72 °C for 13 sec. The specificity of the amplified PCR products was assessed by a melting curve analysis. The crossing-point value (Cp), which is inversely proportional to the initial template copy number, was determined by the Light Cycler Software Program provided by the manufacturer.

2.6. Immunofluorescence microscopy

Immunofluorescence microscopy was performed as described previously [47,48]. HPASMCs were seeded onto 96-well plates at a density of 2×10^3 cells per well. After washing with PBS, the cells were fixed with 2% formaldehyde for 15 min at room temperature, permeabilized in methanol (−20°C, 10 min), and blocked in 1% BSA for 60 min. The cells were then incubated with anti-GLI1 antibodies at 1:100 dilution at 4°C overnight. Following three times washes with PBS, the cells were incubated with secondary antibodies (1:200 dilution) for 1 h at 37°C. The cells were then washed three times (5 min each) in PBS before visualization with the use of a fluorescent microscope (Olympus IX-71) using appropriate excitation and emission spectra at ×200 magnification.

2.7. Protein extraction and Western blotting analysis

The HPASMCs were made quiescent by serum starvation for 24 h and then exposed to hypoxia for the different time periods [49,50]. The cells were washed with cold PBS and lysed in buffer containing 15 mM KCl, 10 mM HEPES, pH 7.6, 2 mM $MgCl_2$, 0.1 mM EDTA, 1 mM DTT, 0.1% Nonidet P-40, 0.5 mM PMSF, 2.5 μg/ml leupeptin, 5 μg/ml antipain and 5 μg/ml aprotinin for 10 min on ice. After centrifugation at $14,000 \times g$ for 20 sec at 4°C, proteins in the nuclei were extracted by incubation at 4°C with vigorous vortex in buffer A containing 420 mM NaCl, 20 mM HEPES, pH 7.9, 0.2 mM EDTA, 25% glycerol, 1 mM DTT, 0.5 mM PMSF, 2.5 μg/ml leupeptin, 5 μg/ml antipain, and 5 μg/ml aprotinin followed by centrifugation at $13,000 \times g$ for 30 min at 4°C. The supernatant extract was collected and stored at −80°C.

Ten μg proteins were separated by SDS–PAGE and blotted onto PVDF membranes as described previously [51,52]. Expression of SHH, PTCH1, GLI1, HIF1α, GAPDH and TATA binding protein (TBP) was determined by immunoblotting using their respective antibodies at dilution of 1:1000, 1:500, 1:600, 1:800, 1:800 and 1:2000 dilution, respectively. Immunoreactive bands were visualized with horseradish peroxidase-conjugated secondary antibodies (1:10,000 dilution). The peroxidase reaction was developed with an enhanced chemiluminescence detection system to visualize the secondary antibodies.

2.8. [³H]-Thymidine incorporation

The HPASMCs were suspended in SMCM containing 2% FBS and 1% SMCGS, seeded in 48-well plates (10^5 cells per well), grown until 80% to 90% confluent, and brought to quiescence by incubation with SMCM containing 0.4% FBS for 24 h. The cells were then treated with hypoxia, SHH, Pur, SAG and cytopamine. For [³H]-thymidine incorporation, 18 h before termination of the cultures, cells were pulsed with 0.5 μCi/well of [³H]-thymidine. After the incubation period, the medium was removed, and the cell monolayer was washed with ice-cold PBS and then detached by incubation with 1 ml of 0.25% trypsin for 5 min. Further tryptic activity was inhibited by addition of 1 ml of DMEM containing 10% FCS. For the measurement of [³H]-thymidine incorporation under the normoxia condition in response to growth factors, the cells were treated for 24 h with 1% smooth muscle cell growth supplement (SMCGS) with or without CyA and Tom. Total DNA containing incorporated [³H]-thymidine was precipitated in cold 7.5% trichloroacetic acid, centrifuged, washed three times with 7.5% trichloroacetic acid, and then counted on an LKB Rackbeta scintillation counter. These experiments were performed for 6 times each in duplicates.

2.9. Apoptosis analysis

Apoptosis was measured by using the Annexin V-propidium iodide binding assay, followed by fluorescence-activated cell sorter (FACS) analysis using a FACScan flow cytometer (Becton Dickinson, Dublin, Ireland). The HPASMCs were designated as viable, apoptotic, or necrotic. The rate of apoptotic cells was detected by the Apoptosis Assay Kit according to the manufacturer's protocol. Briefly, after the cells were harvested, washed in cold PBS and resuspended in annexin-binding buffer, 5 μl FITC-annexin V and 10 μl propidium iodide working solution were added into 195 μl cell suspension. The cells were then incubated for 10 min at room temperature. After the incubation period, 190 μl annexin-binding buffer were added to each sample, gently mixed and kept on ice. The stained cells were analyzed by flow cytometry. Approximately 20,000 counts were made for each sample.

2.10. Statistical analysis

Data are expressed as the means ± SE. Differences were evaluated using One-way ANOVA test, and $P < 0.05$ was considered as statistically significant for all comparisons.

3. Results

3.1. Expression of components of the SHH signaling pathway in the HPASMCs

To determine whether the major components of the SHH signaling pathway, including SHH, PTCH1, SMO, GLI1, GLI2 and GLI3, are expressed in the static HPASMCs, we measured their mRNA expression levels by PCR using GADPH as a control. The mRNA of SHH, PTCH1, SMO, GLI1, GLI2, GLI3 and GAPDH was detected in the HPASMCs (Fig. 1) and the sizes of the PCR products matched with their anticipated sizes of 162, 215, 258, 344, 152, 158 and 450 bp, respectively. These data demonstrate that the SHH signaling components SHH, PTCH1, SMO, GLI1, GLI2 and GLI3 are present in the HPASMCs.

3.2. Hypoxia induces upregulation and secretion of SHH in the HPASMCs

To explore the potential function of the SHH signaling pathway in the HPASMCs, we determined if this pathway could be activated by hypoxia. The expression of SHH in the HPASMCs subjected to hypoxia was quantified by immunoblotting. The expression of SHH normalized to GAPDH was increased 2.2-fold at 4 h hypoxia as compared with the normoxia group ($P < 0.05$). At 8 h after hypoxia, the protein level of SHH further increased by 1.6-fold as compared with the hypoxic 4 h group ($P < 0.05$). At 12 h after hypoxia, the expression of SHH was less than the 8 h group, but still higher than the normoxia group ($P < 0.05$) (Fig. 2A). In contrast, expression of PTCH1 only slightly increased and decreased at 8 and 12 h after hypoxia, respectively (Fig. 2A.)

As SHH is a secreted glycoprotein, we then measured the expression of SHH in the HPASMC culture medium by ELISA. The expression of SHH in the culture medium was also markedly increased by hypoxia (Fig. 2B). Interestingly, the time courses of augmentation in SHH expression and secretion into the culture medium in response to hypoxia were different. Particularly, the expression of SHH in the cells went down at 12 h after hypoxia, whereas SHH secretion into the culture medium reached the highest point at 24 h after hypoxia and remained at the same level at the 48 h hypoxia (Fig. 2B). These data demonstrate that the expression of SHH in the HPASMCs and its secretion into the culture medium are inducible by hypoxia.

To further determine the mechanism of the enhanced expression of SHH protein, the mRNA level of SHH in the HPASMCs after hypoxia was quantified by real-time PCR. The mRNA expression level of SHH in the HPASMCs was clearly increased in response to hypoxia and the time course of the mRNA expression was very similar to that of the cellular SHH protein expression. The mRNA expression of SHH was increased by 2.5-fold at 4 h after hypoxia

compared with the normoxia group ($P < 0.05$). At 8 h after hypoxia, the mRNA level of SHH further increased. At 12 h after hypoxia, the mRNA level of SHH was reduced as compared with the 8 h group, but still higher than the normoxia group ($P < 0.05$) (Fig. 2C). These data demonstrate that hypoxia-mediated upregulation of SHH is likely mediated through regulating the mRNA expression of SHH.

3.3. Hypoxia induces upregulation of HIF1 and its role in the expression of SHH in the HPASMCs

It has also been demonstrated that expression of SHH in response to hypoxia can be inhibited by blocking the function of HIF1α [40,42]. To determine if this is the case in the HPASMCs, we first determined if hypoxia could also induce expression of HIF1. Similar to the SHH expression, HIF1 expression was also markedly increased in response to hypoxia (Fig. 3A). These data suggest that the expression of HIF1 is inducible by hypoxia. We then determined the role of HIF1 in the expression of SHH in the hypoxic HPASMCs. The pretreatment with anti-HIF1α antibodies remarkably inhibited the enhancement of SHH expression induced by hypoxic stimulation (Fig. 3B). These data demonstrate that hypoxia-induced SHH expression is dependent on the normal function of HIF1α in the HPASMCs which is consistent with an essential role of HIF1 in the expression of SHH in other cell types [40,42].

3.4. Hypoxia enhances nuclear translocation of GLI1 in the HPASMCs

We next investigated if hypoxia could induce nuclear translocation of GLI1 in the HPASMCs by two complementary methods, nuclear fractionation followed by immunoblotting and direct visualization of the subcellular distribution of GLI1 by immunofluorescence microscopy. GLI1 expression was markedly increased in the nuclear fraction, but decreased in the cytosolic fraction in the hypoxic HPASMCs as compared with the normoxia group as measured by immunoblotting (Fig. 4A). Consistently, microcopy analysis showed that GLI1 was mainly expressed in the cytoplasm in the normoxia HPASMCs and hypoxia dramatically augmented the expression of GLI1 in the nuclear region (Fig. 4B and 4C). These data suggest that hypoxia induces the nuclear translocation of GLI1.

To further prove that the facilitated nuclear translocation of GLI1 in the HPASMCs in response to hypoxia was indeed induced by the activation of the SHH pathway, we investigated the effect of the treatments with anti-SHH and anti-HIF1 antibodies and CyA, a SMO inhibitor, on the GLI1 nuclear expression. The HPASMCs were pretreated with CyA or the antibodies and then subjected to hypoxia. The treatment with CyA and either antibody markedly suppressed the expression of GLI1 in the nuclear fraction measured by immunoblotting (Fig. 4A) and nuclear translocation of GLI1 visualized by microscopy (Fig. 4B and 4C). In contrast, these treatments did not have clear influence on the nuclear translocation of GLI1 in the normoxia HPASMCs (data not shown). These data demonstrate that GLI1 translocation to the nuclear region in the hypoxic HPASMCs is likely associated with the activation of the SHH signaling pathway.

3.5. Hypoxia-induced cell proliferation and the role of the SHH pathway

It has been well demonstrated that hypoxia induces cell proliferation of rat pulmonary arterial and aortal SMCs [1] as well as a number of other cell types, including neural stem cells, pancreatic stellate cells, murine fibroblasts, cancer cell lines MCF7, RKO, Hela, and HT1080 [2–4]. However, whether or not HPASMCs undergo similar cell proliferation in response to hypoxia has not been determined. Therefore, we next studied the effect of hypoxia on the cell proliferation of the HPASMCs by measuring [^{3}H] thymidine incorporation and counting the cell numbers. [^{3}H] thymidine incorporation (Fig. 5A) and the numbers of HPASMCs (Fig. 5B) were markedly augmented to the same degree (by 90%) after exposure to hypoxia, compared with the normoxia group. These data demonstrate that, similar to pulmonary smooth muscle

cells from other species [53–57], the HPASMCs undergo hypertrophic growth under the stimulation of hypoxia.

We then determined the possible role of the SHH signaling pathway in the cell proliferationof the HPASMCs in response to hypoxic stimulation. The treatments with CyA and anti-SHH and anti-HIF antibodies significantly attenuated the hypoxia-induced $[^3H]$-thymidine incorporation and cell numbers of HPASMCs (Fig. 5A and 5B). In contrast, the treatment with Tom, an inactive compound structurally-related to CyA, did not produce clear inhibitory effects. The treatment with CyA, anti-SHH and anti-HIF antibodies and Tom also did not alter the $[^3H]$-thymidine incorporation and cell numbers of HPASMCs under the normal condition. $[^3H]$ Thymidine incorporation and the cell numbers were also significantly enhanced after stimulation with growth factors which was partially inhibited by treatment with CyA, but not Tom (Fig. 5A and 5B). These data demonstrate that hypoxia-induced HPASMC proliferation is mediated at least in part by activating the SHH pathway.

We sought to determine if the direct activation of the SHH pathway could promote the cell proliferation of HPASMCs. Addition of the recombinant human SHH into the culture medium at a concentration of 1.0 μg/ml significantly increased the cell proliferation of HPASMCs by 2.6-fold as measured by $[^3H]$-thymidine incorporation (Fig. 5C). Activation of the SHH pathway by incubation with Pur (4 μM) and SAG (100 nM), two SMO agonists, also significantly augmented $[^3H]$-thymidine incorporation by 2.8- and 2.2-fold, respectively (Fig. 5C). The increases in the $[^3H]$-thymidine incorporation induced by SHH, Pur and SAG were markedly reversed by CyA, but not Tom (Fig. 5C). These data demonstrate that, similar to hypoxia, the direct activation of the SHH signaling also provokes the cell proliferation of the HPASMCs.

3.5. Enhancement of apoptosis by CyA in the hypoxic HPASMCs

We next examined the role of the SHH signaling pathway in the apoptosis of the HPASMCs in response to hypoxia by flow cytometry after staining with the Annexin V- FITC (Annexin V) and propidium iodide (PI). This method detects the cells in the necrotic (B1), late apoptotic (B2), viable (B3), and early apoptotic states (B4) (Fig. 6A). CyA treatment at a concentration of 20 μM did not clearly influence the apoptosis of normoxia HPASMCs. In contrast, such a treatment significantly enhanced the number of annexin V-positive HPASMCs by 2.4-fold in the hypoxic condition compared with the treatment with Tom (Fig. 6A and 6B). These results demonstrate that the SHH signaling pathway may be involved in the regulation of apoptosis in the HPASMCs once subjected to hypoxia.

4. Discussion

The SHH signaling pathway is a well-known key mediator for many fundamental processes in multiple organs during embryonic development [58,59]. A recent study has demonstrated that the SHH signaling components exist in the adult rat VSMCs and their expression can be modulated by biomechanical stimulation both in vitro and in vivo, suggesting that the SHH pathway may play a role in the arterial remodeling and atherogenesis [60]. However, the role of the SHH pathway in hypoxic pulmonary vascular remodeling has not been studied. In this study, we used the adult HPASMCs as a cell model to explore the possible function of the SHH activation in regulating cell proliferation by hypoxia. We have demonstrated that hypoxia markedly activates the SHH pathway in the HPASMCs and that hypoxia also enhances the proliferation of the HPASMCs which can be reversed by inhibiting the SHH pathway.

We have demonstrated that the HPASMCs contain the main components of the SHH pathway including SHH, SMO, PTCH1 and GLI. More importantly, we have shown that hypoxia augmented SHH expression and secretion into the culture medium. However, it is interesting

to note that the time courses of hypoxia-induced SHH expression and secretion are clearly different. Although the maximal expression of SHH was achieved at 8 h after hypoxia, maximal SHH secretion into the culture medium was observed from 12 to 48 h after hypoxia. One possible mechanism responsible for this discrepancy is that the function of the proteins Dispatched (DISP), which have been demonstrated to control the release of cholesterol-modified HH [61,62], is altered by hypoxia. At 8 h after hypoxia, SHH secretion does not reach the maximal level, which may be caused by the limited expression/function of DISP. It is possible that hypoxia for a longer period of time (e.g. > 8 h) will stimulate the expression/function of DISP, promoting the release of SHH into the culture medium. Nevertheless, our data demonstrate that the expression of SHH in the HPASMCs and its secretion into the culture medium are inducible by hypoxia.

We have also shown that, under the normoxia condition, GLI1 mainly expresses in the cytoplasmic compartment and hypoxia facilitates its translocation to the nuclei in the HPASMCs. The subcellular localization of GLI1 as well as its nuclear translocation in response to the activation of the SHH signaling pathway is still a matter of debate. It has been demonstrated that the distribution of GLI1 in the nuclei and the cytoplasm may be different in different cells and increasing evidence suggest that GLI1 subcellular localization is a highly regulated process [63–66]. Increased GLI1 expression and enhanced nuclear translocation [67] can be used an indicator for the activation of the SHH pathway. Interestingly, it has been demonstrated that the expression of GLI1 is controlled by other GLI proteins [68,69]. Taken together, our data demonstrate that the SHH pathway is activated in the HPASMCs in response to hypoxia, reflected by increased expression and secretion of SHH and the nuclear translocation of GLI1. These data demonstrate for the first time that hypoxia is a strong stimulator for the SHH signaling pathway in the HPASMCs. These data are also consistent with many other reports demonstrating that the SHH pathway can be activated by hypoxia in cardiomyoblast cells, neurons, astrocytes, and neural progenitor cells [35,40–43].

The most exciting data presented in this manuscript is that cell proliferation of the HPASMCs in response to hypoxia is mediated at least in part through the SHH pathway. First, we have demonstrated that hypoxia enhances cell proliferation of the HPASMCs as measured by [^{3}H]-thymidine incorporation and cell numbers. These results are consistent with many other reports demonstrating that hypoxia is a strong proliferation stimulator of pulmonary cells [70–73]. Second, stimulation of the SHH pathway through addition of purified recombinant SHH and administration of SMO agonists also promotes cell proliferation. These results provide direct evidence implicating that the SHH signaling pathway is involved in the regulation of HPASMCs. Third, cell proliferation induced by hypoxia can be inhibited by treatments with cyclopamine, a specific inhibitor of SMO, and anti-SHH antibodies, further suggesting an important role of the activation of SHH pathway in the hypoxia-mediated cell proliferation in the HPASMCs. Future experiments will define the role of SHH-PTCH-GLI pathway in the hypoxia-mediated HPASMC growth in vivo.

Cyclopamine has been well shown to induce apoptosis in many kinds of cancer cells, such as colorectal, pancreas, and small-cell lung cancer [17,31,74]. Therefore, SHH antagonists are being developed for the treatment of several cancers [75]. In addition, removal of the SHH signaling from adult hearts results in cardiomyocyte apoptosis [76]. These suggest a protective role for the SHH signaling pathway. In this report, we have demonstrated that administration of cyclopamine to inhibit the SHH pathway strongly enhanced apoptosis in the HPASMCs specifically under the hypoxia condition. As hypoxia activates the SHH pathway, these data suggest that activation of the SHH is involved in the regulation of apoptosis of the hypoxic HPASMCs. These results provide important evidence implying that the SHH antagonists may be used as therapeutic agents for hypoxia-induced diseases.

Acknowledgments

References

1. Chan SY, Loscalzo J. Pathogenic mechanisms of pulmonary arterial hypertension. J Mol Cell Cardiol 2008;44:14–30. [PubMed: 17950310]

2. Mecham RP, Whitehouse LA, Wrenn DS, Parks WC, Griffin GL, Senior RM, Crouch EC, Stenmark KR, Voelkel NF. Smooth muscle-mediated connective tissue remodeling in pulmonary hypertension. Science 1987;237:423–426. [PubMed: 3603030]

3. Stenmark KR, Fagan KA, Frid MG. Hypoxia-induced pulmonary vascular remodeling: cellular and molecular mechanisms. Circ Res 2006;99:675–691. [PubMed: 17008597]

4. Orlandi A, Bochaton-Piallat ML, Gabbiani G, Spagnoli LG. Aging, smooth muscle cells and vascular pathobiology: implications for atherosclerosis. Atherosclerosis 2006;188:221–230. [PubMed: 16487530]

5. Voelkel NF, Douglas IS, Nicolls M. Angiogenesis in chronic lung disease. Chest 2007;131:874–879. [PubMed: 17356107]

6. Gerthoffer WT. Mechanisms of vascular smooth muscle cell migration. Circ Res 2007;100:607–621. [PubMed: 17363707]

7. Humbert M, Montani D, Perros F, Dorfmuller P, Adnot S, Eddahibi S. Endothelial cell dysfunction and cross talk between endothelium and smooth muscle cells in pulmonary arterial hypertension. Vascul Pharmacol 2008;49:113–118. [PubMed: 18606248]

8. Mitchell RN, Libby P. Vascular remodeling in transplant vasculopathy. Circ Res 2007;100:967–978. [PubMed: 17431198]

9. Cooper AL, Beasley D. Hypoxia stimulates proliferation and interleukin-1alpha production in human vascular smooth muscle cells. Am J Physiol Heart Circ Physiol 1999;277:H1326–1337.

10. Horiuchi M, Cui TX, Li Z, Li JM, Nakagami H, Iwai M. Fluvastatin enhances the inhibitory effects of a selective angiotensin II type 1 receptor blocker, valsartan, on vascular neointimal formation. Circulation 2003;107:106–112. [PubMed: 12515751]

11. Seki Y, Kai H, Shibata R, Nagata T, Yasukawa H, Yoshimura A, Imaizumi T. Role of the JAK/STAT pathway in rat carotid artery remodeling after vascular injury. Circ Res 2000;87:12–18. [PubMed: 10884366]

12. Radhakrishnan Y, Maile LA, Ling Y, Graves LM, Clemmons DR. Insulin-like growth factor-I stimulates Shc-dependent phosphatidylinositol 3-kinase activation via Grb2-associated p85 in vascular smooth muscle cells. J Biol Chem 2008;283:16320–16331. [PubMed: 18420583]

13. Rosner D, Stoneman V, Littlewood T, McCarthy N, Figg N, Wang Y, Tellides G, Bennett M. Interferon-gamma induces Fas trafficking and sensitization to apoptosis in vascular smooth muscle cells via a PI3K- and Akt-dependent mechanism. Am J Pathol 2006;168:2054–2063. [PubMed: 16723718]

14. Chen KH, Guo X, Ma D, Guo Y, Li Q, Yang D, Li P, Qiu X, Wen S, Xiao RP, Tang J. Dysregulation of HSG triggers vascular proliferative disorders. Nat Cell Biol 2004;6:872–883. [PubMed: 15322553]

15. Campbell M, Trimble ER. Modification of PI3K- and MAPK-dependent chemotaxis in aortic vascular smooth muscle cells by protein kinase CbetaII. Circ Res 2005;96:197–206. [PubMed: 15591231]

16. Taipale J, Cooper MK, Maiti T, Beachy PA. Patched acts catalytically to suppress the activity of Smoothened. Nature 2002;418:892–897. [PubMed: 12192414]

17. Watkins DN, Peacock CD. Hedgehog signalling in foregut malignancy. Biochem Pharmacol 2004;68:1055–1060. [PubMed: 15313401]

18. Jenkins D. Hedgehog signalling: emerging evidence for non-canonical pathways. Cell Signal 2009;21:1023–1034. [PubMed: 19399989]

19. Eaton S. Multiple roles for lipids in the Hedgehog signalling pathway. Nat Rev Mol Cell Biol 2008;9:437–445. [PubMed: 18500255]

20. Claret S, Sanial M, Plessis A. Evidence for a novel feedback loop in the Hedgehog pathway involving Smoothened and Fused. Curr Biol 2007;17:1326–1333. [PubMed: 17658259]

21. Meloni AR, Fralish GB, Kelly P, Salahpour A, Chen JK, Wechsler-Reya RJ, Lefkowitz RJ, Caron MG. Smoothened signal transduction is promoted by G protein-coupled receptor kinase 2. Mol Cell Biol 2006;26:7550–7560. [PubMed: 16908539]

22. Riobo NA, Saucy B, DiLizio C, Manning DR. Activation of heterotrimeric G proteins by Smoothened. Proceedings of the National Academy of Sciences 2006;103:12607–12612.

23. Jiang J. Regulation of Hh/Gli signaling by dual ubiquitin pathways. Cell Cycle 2006;5:2457–2463. [PubMed: 17102630]

24. Matise MP. Order in the classroom: graded responses to instructive Hh signaling in the CNS. Cell Cycle 2007;6:1194–1199. [PubMed: 17495537]

25. Ruiz i Altaba A, Palma V, Dahmane N. Hedgehog-Gli signalling and the growth of the brain. Nat Rev Neurosci 2002;3:24–33. [PubMed: 11823802]

26. Beachy PA, Karhadkar SS, Berman DM. Tissue repair and stem cell renewal in carcinogenesis. Nature 2004;432:324–331. [PubMed: 15549094]

27. Amankulor NM, Hambardzumyan D, Pyonteck SM, Becher OJ, Joyce JA, Holland EC. Sonic hedgehog pathway activation is induced by acute brain injury and regulated by injury-related inflammation. J Neurosci 2009;29:10299–10308. [PubMed: 19692604]

28. Singh RR, Cho-Vega JH, Davuluri Y, Ma S, Kasbidi F, Milito C, Lennon PA, Drakos E, Medeiros LJ, Luthra R, Vega F. Sonic Hedgehog Signaling Pathway Is Activated in ALK-Positive Anaplastic Large Cell Lymphoma. Cancer Res 2009;69:2550–2558. [PubMed: 19244133]

29. Plaisant M, Fontaine C, Cousin W, Rochet N, Dani C, Peraldi P. Activation of hedgehog signaling inhibits osteoblast differentiation of human mesenchymal stem cells. Stem Cells 2009;27:703–713. [PubMed: 19096040]

30. Yu M, Gipp J, Yoon JW, Iannaccone P, Walterhouse D, Bushman W. Sonic hedgehog-responsive genes in the fetal prostate. J Biol Chem 2009;284:5620–5629. [PubMed: 19095649]

31. Thayer SP, di Magliano MP, Heiser PW, Nielsen CM, Roberts DJ, Lauwers GY, Qi YP, Gysin S, Castillo CF-d, Yajnik V, Antoniu B, McMahon M, Warshaw AL, Hebrok M. Hedgehog is an early and late mediator of pancreatic cancer tumorigenesis. Nature 2003;425:851–856. [PubMed: 14520413]

32. Ingham PW, McMahon AP. Hedgehog signaling in animal development: paradigms and principles. Genes Dev 2001;15:3059–3087. [PubMed: 11731473]

33. Morrow D, Cullen JP, Liu W, Guha S, Sweeney C, Birney YA, Collins N, Walls D, Redmond EM, Cahill PA. Sonic Hedgehog induces Notch target gene expression in vascular smooth muscle cells via VEGF-A. Arterioscler Thromb Vasc Biol 2009;29:1112–1118. [PubMed: 19407245]

34. Surace EM, Balaggan KS, Tessitore A, Mussolino C, Cotugno G, Bonetti C, Vitale A, Ali RR, Auricchio A. Inhibition of ocular neovascularization by hedgehog blockade. Mol Ther 2006;13:573–579. [PubMed: 16343995]

35. Sims JR, Lee SW, Topalkara K, Qiu J, Xu J, Zhou Z, Moskowitz MA. Sonic hedgehog regulates ischemia/hypoxia-induced neural progenitor proliferation. Stroke 2009;40:3618–3626. [PubMed: 19762700]

36. Pola R, Ling LE, Aprahamian TR, Barban E, Bosch-Marce M, Curry C, Corbley M, Kearney M, Isner JM, Losordo DW. Postnatal Recapitulation of Embryonic Hedgehog Pathway in Response to Skeletal Muscle Ischemia. Circulation 2003;108:479–485. [PubMed: 12860919]

37. Merchant A, Joseph G, Wang Q, Brennan S, Matsui W. Gli1 regulates the proliferation and differentiation of HSCs and myeloid progenitors. Blood 115:2391–2396. [PubMed: 20107231]

38. Rutter M, Wang J, Huang Z, Kuliszewski M, Post M. Gli2 influences proliferation in the developing lung through regulation of cyclin expression. Am J Respir Cell Mol Biol 42:615–625. [PubMed: 19574535]

39. Kim Y, Yoon JW, Xiao X, Dean NM, Monia BP, Marcusson EG. Selective down-regulation of glioma-associated oncogene 2 inhibits the proliferation of hepatocellular carcinoma cells. Cancer Res 2007;67:3583–3593. [PubMed: 17440069]

40. Hwang JM, Weng YJ, Lin JA, Bau DT, Ko FY, Tsai FJ, Tsai CH, Wu CH, Lin PC, Huang CY, Kuo WW. Hypoxia-induced compensatory effect as related to Shh and HIF-1alpha in ischemia embryo rat heart. Mol Cell Biochem 2008;311:179–187. [PubMed: 18228117]

41. Dokucu AI, Ozturk H, Tuncer MC, Yilmaz F. The effects of molsidomine on hypoxia inducible factor alpha and Sonic hedgehog in testicular ischemia/reperfusion injury in rats. Int Urol Nephrol 2009;41:101–108. [PubMed: 18787973]

42. Bijlsma MF, Groot AP, Oduro JP, Franken RJ, Schoenmakers SH, Peppelenbosch MP, Spek CA. Hypoxia induces a hedgehog response mediated by HIF-1alpha. J Cell Mol Med 2009;13:2053–2060. [PubMed: 18774959]

43. Ozturk H, Tuncer MC, Buyukbayram H. Nitric oxide regulates expression of sonic hedgehog and hypoxia-inducible factor-1alpha in an experimental model of kidney ischemia-reperfusion. Ren Fail 2007;29:249–256. [PubMed: 17497436]

44. Semenza GL. Targeting HIF-1 for cancer therapy. Nat Rev Cancer 2003;3:721–732. [PubMed: 13130303]

45. Lee KA, Roth RA, LaPres JJ. Hypoxia, drug therapy and toxicity. Pharmacol Ther 2007;113:229–246. [PubMed: 17046066]

46. Wang GS, Qian GS, Zhou DS, Zhao JQ. JAK-STAT signaling pathway in pulmonary arterial smooth muscle cells is activated by hypoxia. Cell Biology International 2005;29:598–603. [PubMed: 15939634]

47. Zhang X, Wang G, Dupre DJ, Feng Y, Robitaille M, Lazartigues E, Feng YH, Hebert TE, Wu G. Rab1 GTPase and dimerization in the cell surface expression of angiotensin II type 2 receptor. J Pharmacol Exp Ther 2009;330:109–117. [PubMed: 19357319]

48. Filipeanu CM, Zhou F, Claycomb WC, Wu G. Regulation of the cell surface expression and function of angiotensin II type 1 receptor by Rab1-mediated endoplasmic reticulum-to-Golgi transport in cardiac myocytes. J Biol Chem 2004;279:41077–41084. [PubMed: 15252015]

49. Wang G, Qian P, Jackson FR, Qian G, Wu G. Sequential activation of JAKs, STATs and xanthine dehydrogenase/oxidase by hypoxia in lung microvascular endothelial cells. Int J Biochem Cell Biol 2008;40:461–470. [PubMed: 17920330]

50. Feng YH, Wang L, Wang Q, Li X, Zeng R, Gorodeski GI. ATP stimulates GRK-3 phosphorylation and beta-arrestin-2-dependent internalization of P2X7 receptor. Am J Physiol Cell Physiol 2005;288:C1342–1356. [PubMed: 15728711]

51. Duvernay MT, Zhou F, Wu G. A conserved motif for the transport of G protein-coupled receptors from the endoplasmic reticulum to the cell surface. J Biol Chem 2004;279:30741–30750. [PubMed: 15123661]

52. Wu G, Zhao G, He Y. Distinct pathways for the trafficking of angiotensin II and adrenergic receptors from the endoplasmic reticulum to the cell surface: Rab1-independent transport of a G protein-coupled receptor. J Biol Chem 2003;278:47062–47069. [PubMed: 12970354]

53. Liang W, Ray JB, He JZ, Backx PH, Ward ME. Regulation of proliferation and membrane potential by chloride currents in rat pulmonary artery smooth muscle cells. Hypertension 2009;54:286–293. [PubMed: 19581510]

54. Dempsey EC, Wick MJ, Karoor V, Barr EJ, Tallman DW, Wehling CA, Walchak SJ, Laudi S, Le M, Oka M, Majka S, Cool CD, Fagan KA, Klemm DJ, Hersh LB, Gerard NP, Gerard C, Miller YE. Neprilysin null mice develop exaggerated pulmonary vascular remodeling in response to chronic hypoxia. Am J Pathol 2009;174:782–796. [PubMed: 19234135]

55. Paddle BM, Wong VK, Muller BD. The cytotoxic effect of anthrax lethal toxin on human lung cells in vitro and the protective action of bovine antibodies to PA and LF. J Appl Toxicol 2006;26:162–168. [PubMed: 16278807]

56. Yu L, Quinn DA, Garg HG, Hales CA. Cyclin-dependent kinase inhibitor p27Kip1, but not p21WAF1/Cip1, is required for inhibition of hypoxia-induced pulmonary hypertension and remodeling by heparin in mice. Circ Res 2005;97:937–945. [PubMed: 16195480]

57. Stiebellehner L, Frid MG, Reeves JT, Low RB, Gnanasekharan M, Stenmark KR. Bovine distal pulmonary arterial media is composed of a uniform population of well-differentiated smooth muscle cells with low proliferative capabilities. Am J Physiol Lung Cell Mol Physiol 2003;285:L819–828. [PubMed: 12857671]

58. Byrd N, Becker S, Maye P, Narasimhaiah R, St-Jacques B, Zhang X, McMahon J, McMahon A, Grabel L. Hedgehog is required for murine yolk sac angiogenesis. Development 2002;129:361–372. [PubMed: 11807029]

59. Dyer MA, Farrington SM, Mohn D, Munday JR, Baron MH. Indian hedgehog activates hematopoiesis and vasculogenesis and can respecify prospective neurectodermal cell fate in the mouse embryo. Development 2001;128:1717–1730. [PubMed: 11311154]

60. Morrow D, Sweeney C, Birney YA, Guha S, Collins N, Cummins PM, Murphy R, Walls D, Redmond EM, Cahill PA. Biomechanical regulation of hedgehog signaling in vascular smooth muscle cells in vitro and in vivo. Am J Physiol Cell Physiol 2007;292:C488–496. [PubMed: 16943241]

61. Burke R, Nellen D, Bellotto M, Hafen E, Senti KA, Dickson BJ, Basler K. Dispatched, a novel sterol-sensing domain protein dedicated to the release of cholesterol-modified hedgehog from signaling cells. Cell 1999;99:803–815. [PubMed: 10619433]

62. Caspary T, Garcia-Garcia MJ, Huangfu D, Eggenschwiler JT, Wyler MR, Rakeman AS, Alcorn HL, Anderson KV. Mouse Dispatched homolog1 is required for long-range, but not juxtacrine, Hh signaling. Curr Biol 2002;12:1628–1632. [PubMed: 12372258]

63. Dahmane N, Lee J, Robins P, Heller P, Ruiz i Altaba A. Activation of the transcription factor Gli1 and the Sonic hedgehog signalling pathway in skin tumours. Nature 1997;389:876–881. [PubMed: 9349822]

64. Lee J, Platt KA, Censullo P, Ruiz i Altaba A. Gli1 is a target of Sonic hedgehog that induces ventral neural tube development. Development 1997;124:2537–2552. [PubMed: 9216996]

65. Kinzler KW, Bigner SH, Bigner DD, Trent JM, Law ML, O'Brien SJ, Wong AJ, Vogelstein B. Identification of an amplified, highly expressed gene in a human glioma. Science 1987;236:70–73. [PubMed: 3563490]

66. Stein U, Eder C, Karsten U, Haensch W, Walther W, Schlag PM. GLI gene expression in bone and soft tissue sarcomas of adult patients correlates with tumor grade. Cancer Res 1999;59:1890–1895. [PubMed: 10213497]

67. Stecca B, Ruiz i Altaba A. A GLI1-p53 inhibitory loop controls neural stem cell and tumour cell numbers. EMBO J 2009;28:663–676. [PubMed: 19214186]

68. Hu MC, Mo R, Bhella S, Wilson CW, Chuang PT, Hui CC, Rosenblum ND. GLI3-dependent transcriptional repression of Gli1, Gli2 and kidney patterning genes disrupts renal morphogenesis. Development 2006;133:569–578. [PubMed: 16396903]

69. McDermott A, Gustafsson M, Elsam T, Hui CC, Emerson CP Jr, Borycki AG. Gli2 and Gli3 have redundant and context-dependent function in skeletal muscle formation. Development 2005;132:345–357. [PubMed: 15604102]

70. Weir EK, Olschewski A. Role of ion channels in acute and chronic responses of the pulmonary vasculature to hypoxia. Cardiovasc Res 2006;71:630–641. [PubMed: 16828723]

71. Clerici C, Planes C. Gene regulation in the adaptive process to hypoxia in lung epithelial cells. Am J Physiol Lung Cell Mol Physiol 2009;296:L267–274. [PubMed: 19118091]

72. Pak O, Aldashev A, Welsh D, Peacock A. The effects of hypoxia on the cells of the pulmonary vasculature. Eur Respir J 2007;30:364–372. [PubMed: 17666559]

73. Vaporidi K, Tsatsanis C, Georgopoulos D, Tsichlis PN. Effects of hypoxia and hypercapnia on surfactant protein expression proliferation and apoptosis in A549 alveolar epithelial cells. Life Sci 2005;78:284–293. [PubMed: 16125734]

74. Qualtrough D, Buda A, Gaffield W, Williams AC, Paraskeva C. Hedgehog signalling in colorectal tumour cells: induction of apoptosis with cyclopamine treatment. Int J Cancer 2004;110:831–837. [PubMed: 15170664]

75. Rubin LL, de Sauvage FJ. Targeting the Hedgehog pathway in cancer. Nat Rev Drug Discov 2006;5:1026–1033. [PubMed: 17139287]

76. Lavine KJ, Kovacs A, Ornitz DM. Hedgehog signaling is critical for maintenance of the adult coronary vasculature in mice. The Journal of Clinical Investigation 2008;118:2404–2414. [PubMed: 18568073]
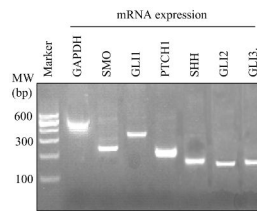
Fig. 1.
mRNA expression of SHH, PTCH1, SMO, GLI1, GLI2 and GLI3 in the HPASMCs as determined by RT-PCR. The expression of GAPDH is used a positive control. Similar results ere obtained in at least three separate experiments. Molecular mass (bp) is indicated at the left.
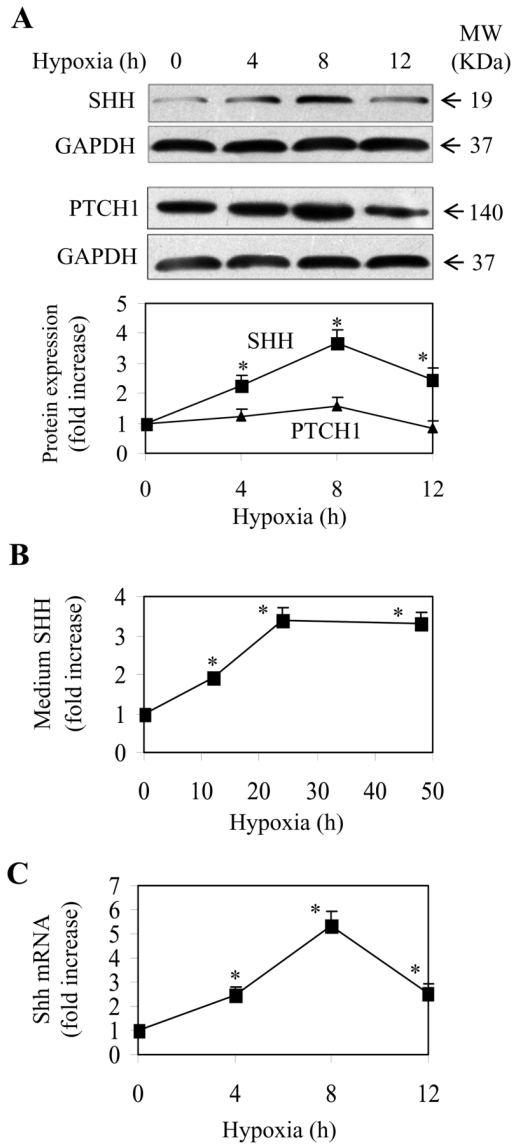
Fig. 2.
Enhancement of SHH expression at the protein and mRNA levels in the HPASMCs in response to hypoxia. (A) SHH and PTCH1 protein expression in the normoxic and hypoxic HPASMCs. The HPASMCs were exposed to hypoxia for 4, 8 and 12 h and SHH and PTCH1 expression was determined by immunoblotting using anti-SHH and anti-PTCH1 antibodies, respectively. Representative Western blots are shown and GAPDH expression is used a sample loading control. Bottom panel: quantitative data of SHH and PTCH1 expression normalized to GAPDH in the HPASMCs. Molecular mass is indicated at the right. (B) SHH protein expression in the culture medium of the HPASMCs after hypoxia for 12, 24 and 48 h measured by ELISA. The values are presented as the means ± S.E. of six independent experiments. C, Expression of SHH mRNA in the HPASMCs after hypoxia as determined by RT-PCR. The values are presented as the means ± S.E. of three independent experiments. $^{*}P < 0.05$ compared the normoxic group (time 0).
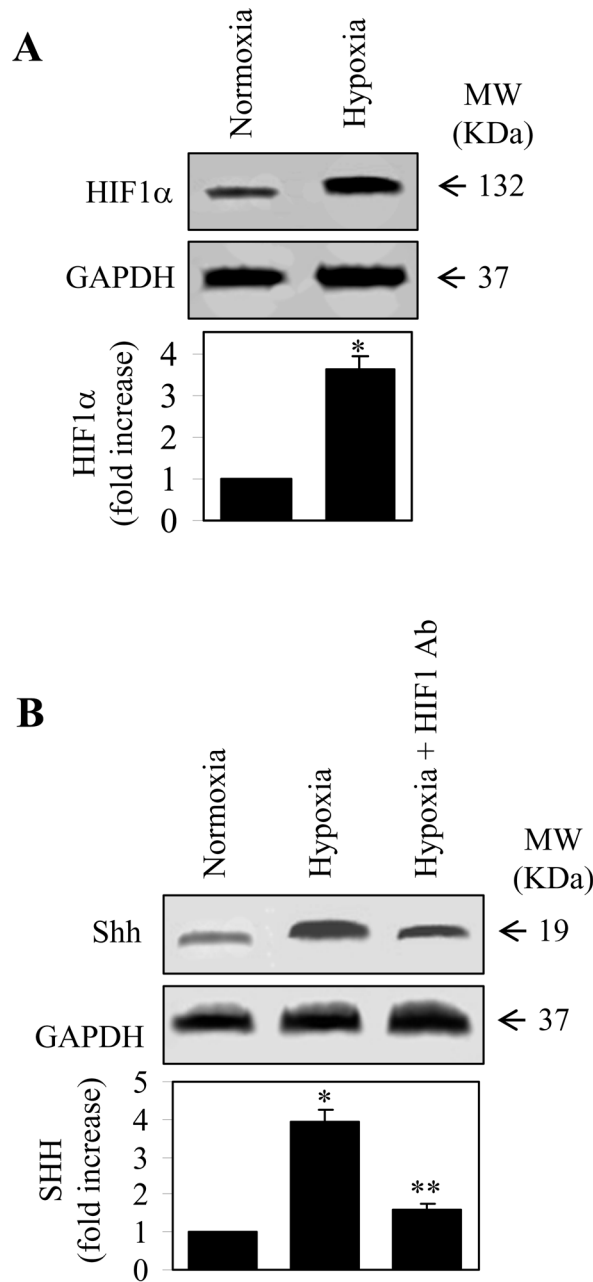
A

B

Fig. 3.
Augmentation of HIF1α expression and attenuation of SHH expression by anti-HIF1α antibodies in the HPASMCs in response to hypoxia. (A) HIF1α expression in the normoxic and hypoxic HPASMCs. The HPASMCs were exposed to hypoxia for 8 h and HIF1α expression was determined by immunoblotting using anti-HIF1α antibodies. Upper panel: a representative Western blot showing HIF1α expression; Middle panel: GAPDH expression as a control; Lower panel: quantitative data of HIF1α expression normalized to GAPDH in the HPASMCs. Molecular mass is indicated at the right. (B) Inhibition of hypoxia-induced SHH expression by pretreatment with anti-HIF1α antibodies. The HPASMCs were subjected to hypoxia for 8 h with or without pretreatment with anti-HIF1α antibodies at a concentration of 1 μg/ml for 24 h and SHH expression was determined by immunoblotting using anti-SHH

antibodies. Upper panel: a representative Western blot showing SHH expression; Middle panel: GAPDH expression as a control; Lower panel: quantitative data of SHH expression normalized to GAPDH in the HPASMCs. Molecular mass is indicated at the right. The values in A and B are presented as the means ± S.E. of three independent experiments. [*] and [**]$P < 0.05$ compared the normoxia and hypoxia groups, respectively.
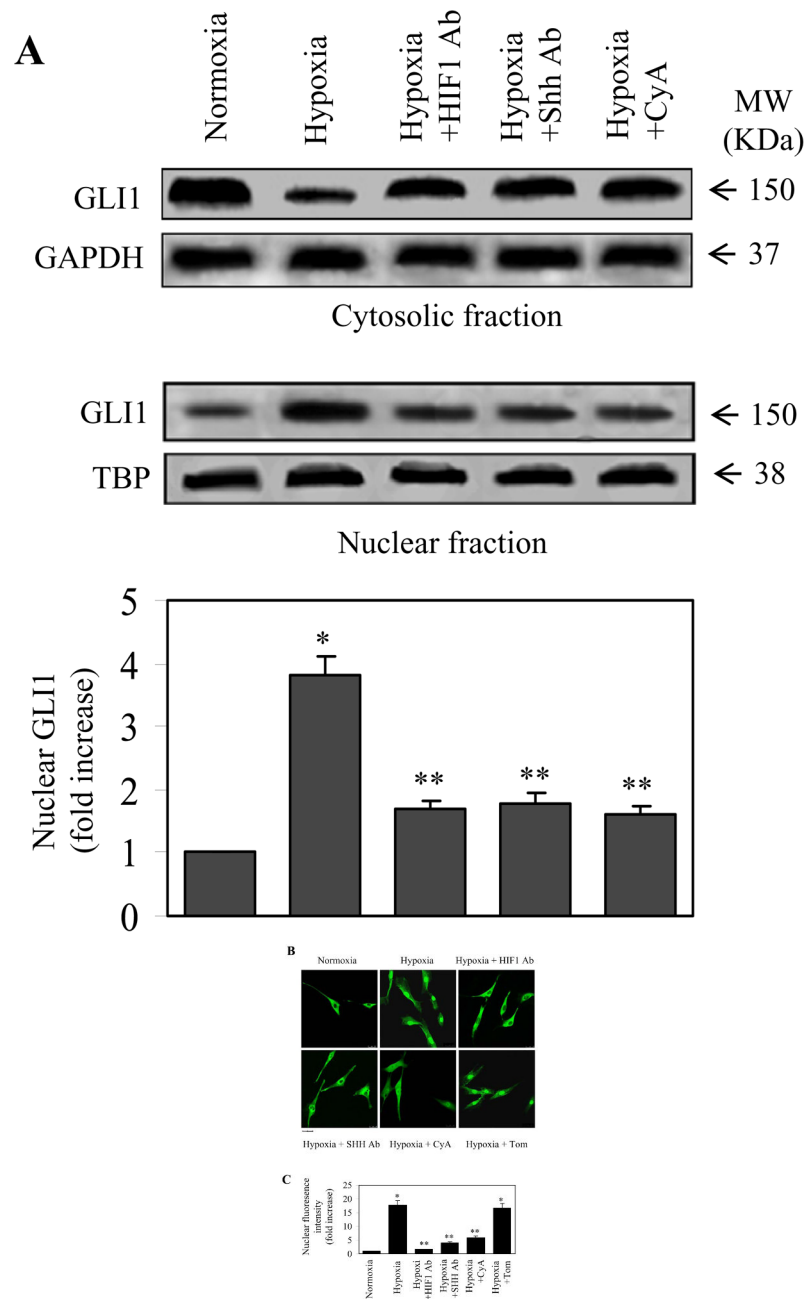
A

Cytosolic fraction

Nuclear fraction

Fig. 4.
Nuclear translocation of GLI1 in the HPASMCs after hypoxia and its inhibition by pretreatment with anti-SHH and anti-HIF1α antibodies and CyA. The HPASMCs were subjected to hypoxia for 24 h with or without pretreatment with antibodies at a concentration of 1 μg/ml for 24 h or CyA at 10 μM for 2 h. (A) GLI1 expression in the cytosolic and nuclear fractions. The nuclear proteins were extracted from the HPASMCs and the amount of GLI1 in the nuclear and cytosolic fractions was determined by immunoblotting using anti-GLI1 antibodies. Expression of GAPDH and TATA binding protein (TBP) was used a sample loading control for cytosolic and nuclear proteins, respectively. Molecular mass is indicated at the left. The bottom panel is the quantitative data of the nuclear GLI1 expression. (B) Representative images showing the nuclear translocation of GLI1 in the HPASMCs after hypoxia and the effect of pretreatments

with anti-SHH and HIF1α antibodies and CyA. The images were taken by immunofluorescence microscopy following staining with anti-GLI1 antibodies as described under the "Experimental procedures". Scale bar, 20 μM. (C) Quantitative data of the fluorescence intensity of GLI1 protein expression in the nuclear region of the HPASMCs (n = 60 cells). In (A) and (C), the quantitative data are presented as the means ± S.E. of three independent experiments. [*] and [**] $p<0.05$ compared the normoxia and hypoxia groups, respectively.
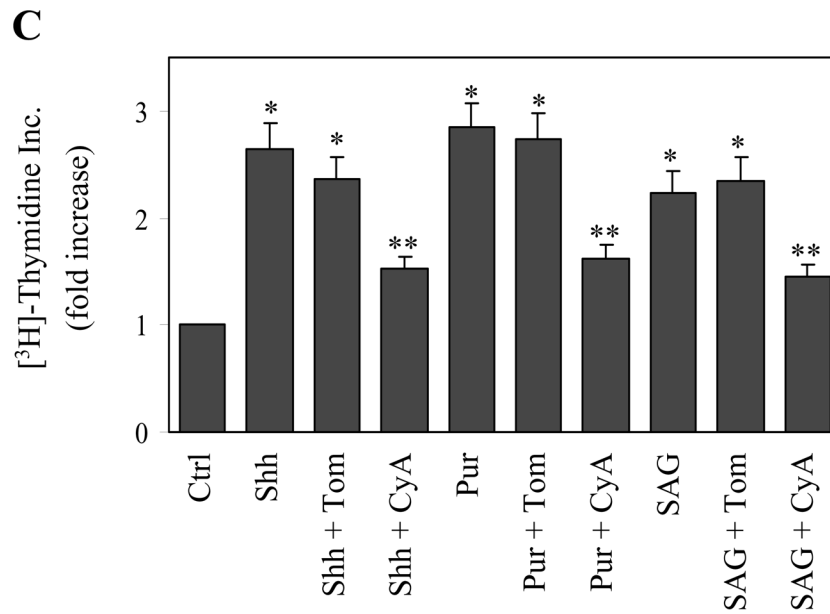
A

B
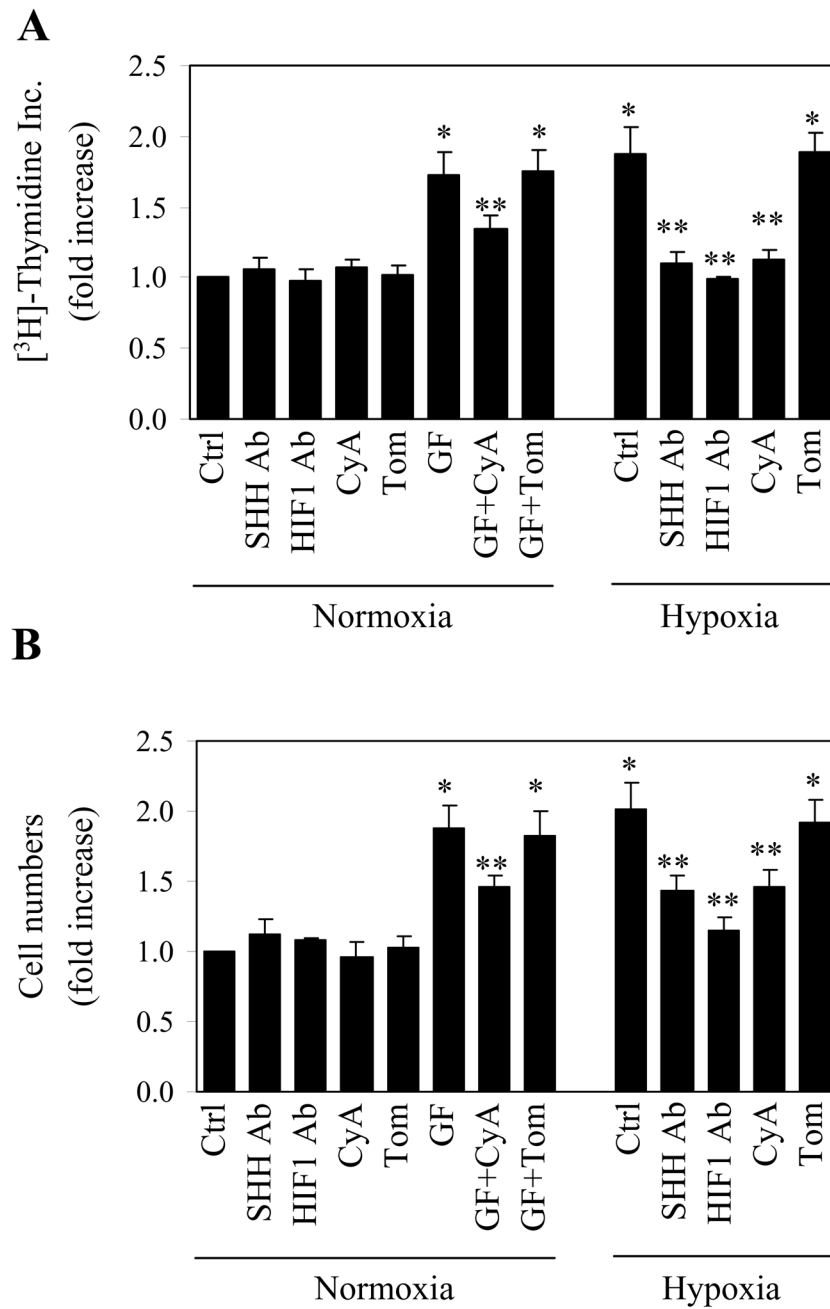
Fig. 5.
Hypoxia-induced cell proliferation of the HPASMCs and its inhibition by pretreatments with anti-SHH and anti-HIF1α antibodies and CyA. The HPASMCs were starved for 24 h, treated with anti-SHH or anti-HIF1α antibodies (1 μg/ml), growth factors (GF), CyA (10μM) or Tom (10μM) and then subjected to hypoxia. Cell proliferation was measured by [^{3}H]-thymidine incorporation (A) and counting cell numbers (B) as described in the "Experimental procedures". The value of [^{3}H]-thymidine incorporation at the basal level (Ctrl) is 760 ± 70 cpm per well. The values are expressed as the means $\pm$ S.E. of four independent experiments. * and ** $P < 0.05$ compared the normoxic and hypoxic groups, respectively. C. Cell proliferation induced by SHH, Pur and SAG in the HPASMCs. The HPASMCs were incubated with SHH at a concentration of 1.0 μg/ml for 24 h or treated with Pur (4 μM) or SAG (100 nM) in the presence or absence of CyA or Tom. Cell proliferation was evaluated by [^{3}H]-thymidine incorporation as described in the "Experimental procedures". The values are presented as the means $\pm$ S.E. of four independent experiments. * and ** $P < 0.05$ versus controls in the normoxia and hypoxia groups, respectively.
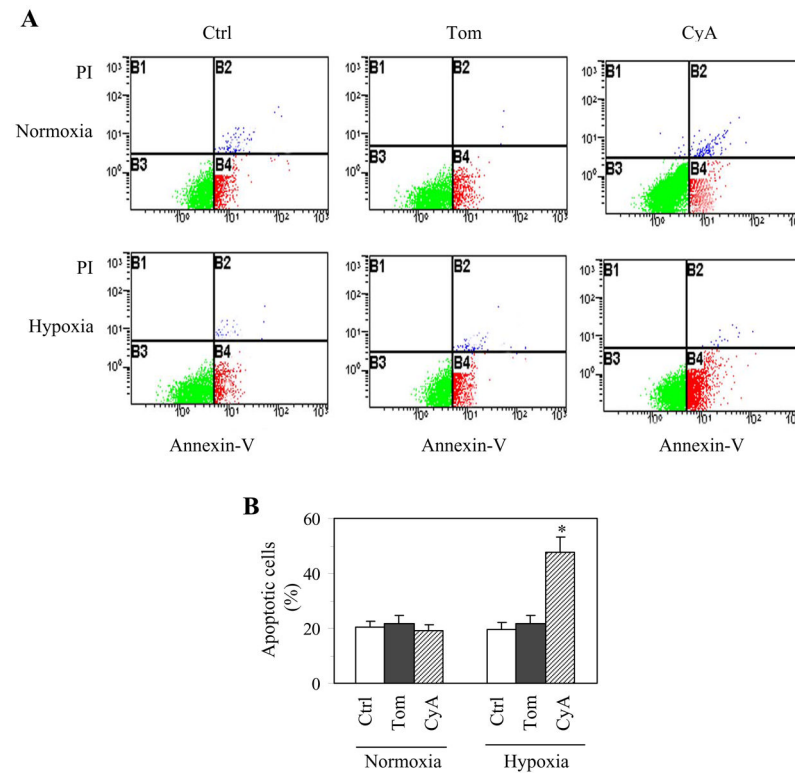
Fig. 6.
Apoptosis induced by CyA in the HPASMCs. (A) Effect of CyA on the apoptosis of HPASMCs exposed to hypoxia. The HPASMCs were starved for 24 h, treated with ethanol (0.1%, Ctrl), CyA (10μM) or Tom (10μM) and then subjected to hypoxia. Apoptosis was measured by flow cytometry following staining with the Annexin V - FITC (Annexin V) and propidium iodide (PI). The lower left quadrants of each panel show the viable cells, which exclude PI and are negative for AV binding (B3, AV$^-$/PI$^-$). The lower right quadrants represent the apoptotic cell, positive for AV binding and negative for PI uptake (B4, AV$^+$/PI$^-$). The upper quadrants (left and right) represent the necrotic cells, positive for PI uptake with or without AV fluorescence. B1, fluorescence height of AV; B2, fluorescence height of PI. Data was taken from one out of six determinations in a typical experiment. Three such experiments were performed. (B) Quantitative data of the apoptotic cells in the B4 section presented as the means ± S.E. of four independent experiments. *P < 0.05 compared with control (Ctrl) in the hypoxic group.